**Atmospheric
Chemistry
and Physics
Discussions**

Effects of temperature and other atmospheric conditions on long-term gaseous mercury observations in the Arctic

A. S. Cole and A. Steffen

Air Quality Research Division, Environment Canada, 4905 Dufferin St., Toronto, Ontario M3H 5T4, Canada

Correspondence to: A. S. Cole (amanda.cole@ec.gc.ca)

ACPD

9, 27167–27194, 2009

Temperature effects on Arctic gaseous mercury

A. S. Cole and A. Steffen

Title Page

Abstract	Introduction
Conclusions	References
Tables	Figures

|◄ | ►|
◄ | ►
Back | Close

Full Screen / Esc

Printer-friendly Version

Interactive Discussion

Temperature effects on Arctic gaseous mercury

A. S. Cole and A. Steffen

Abstract

Gaseous elemental mercury (GEM) measurements at Alert, Canada, from 1995 to 2007 were analyzed for statistical time trends and for correlations with meteorological and climate data. A significant decreasing trend in annual GEM concentration is reported at Alert, with an estimated slope of $-0.0086\,\mathrm{ng\,m^{-3}\,yr^{-1}}$ ($-0.6\%\,\mathrm{yr^{-1}}$) over this 13-year period. It is shown that there has been a shift in the month of minimum mean GEM concentration from May to April due to a change in the timing of springtime atmospheric mercury depletion events (AMDEs). These AMDEs are found to decrease with increasing local temperature within each month, both at Alert and at Amderma, Russia. These results agree with the temperature dependence suggested by previous experimental results and theoretical kinetic calculations and highlight the potential for changes in Arctic mercury chemistry with climate. A correlation between total monthly AMDEs at Alert and the Polar/Eurasian Teleconnection Index was observed only in March, perhaps due to higher GEM inputs in early spring in those years with a weak polar vortex. A correlation of AMDEs at Alert with wind direction supports the origin of mercury depletion events over the Arctic Ocean, in agreement with a previous trajectory study of ozone depletion events. Interannual variability in total monthly depletion event frequency at Alert does not appear to correlate significantly with total or first-year northern hemispheric sea ice area or with other major teleconnection patterns. Nor do AMDEs at either Alert or Amderma correlate with local wind speed, as might be expected if depletion events are sustained by stable, low-turbulence atmospheric conditions. The data presented here – both the change in timing of depletion events and their relationship with temperature – can be used as additional constraints to improve the ability of global models to predict the cycling and deposition of mercury in the Arctic.

1   Introduction

Mercury in the Arctic is of particular interest for two reasons. From a health perspective, mercury is found in high levels in Arctic wildlife and in some populations despite there being no major mercury sources nearby. For atmospheric scientists, monitoring of atmospheric mercury revealed unusual "atmospheric mercury depletion events" (AMDEs) in which mercury concentrations drop precipitously on timescales of a few hours (Schroeder et al., 1998). Based on research to date, these AMDEs are believed to be due to chemical oxidation by halogen radicals of long-lived gaseous elemental mercury (GEM, or Hg^0) to much more quickly deposited reactive gaseous mercury compounds (RGM) and particle-bound mercury (PHg), and are estimated to contribute as much as 30–55% of the total atmospheric mercury deposited to the Arctic annually (Ariya et al., 2004; Christensen et al., 2004; Skov et al., 2004; Dastoor et al., 2008). As the Arctic undergoes dramatic change due to reduced sea ice and warming temperatures (Cosimo, 2006), it is crucial to understand how climate change may affect the frequency and magnitude of AMDEs in the future in order to predict future inputs of mercury to polar regions.

There is already some evidence suggesting that mercury oxidation chemistry is influenced directly and indirectly by climate. Theoretical calculations predict that the net oxidation of Hg^0 to $HgBr_2$ by bromine radicals – a likely oxidation pathway during AMDEs – will be much faster at low temperatures (Goodsite et al., 2004). The origin of high levels of these bromine radicals ("bromine explosions") appears to be heterogeneous reactions with bromide ions (Br^-) in snow, ice and/or aerosol, where sea salt is the original source of bromide (Vogt et al., 1996; Fan and Jacob, 1992). These reactions are likely temperature-dependent, as shown by laboratory experiments on ice (Adams et al., 2002) and predicted by calculations accounting for low-temperature acidification of sea-salt aerosol (Sander et al., 2006). Additionally, bromine explosions, and by extension both ozone depletion events and AMDEs, may be tied to snow and ice characteristics through frost flowers (Kaleschke et al., 2004), first-year sea ice (Simp-

Temperature effects on Arctic gaseous mercury

A. S. Cole and A. Steffen

son et al., 2007), and inland snow pack chemistry (Simpson et al., 2005; Piot and von Glasow, 2008), all of which would be sensitive to climate change. Finally, a short field study at McMurdo, Antarctica, showed a correlation between GEM and air temperature although it was not clear if temperature was the direct cause of the GEM variability (Brooks et al., 2008). However, there has not yet been an analysis directly linking mercury depletion events and temperature during long-term monitoring.

In addition to the springtime low GEM concentrations, the Arctic regularly experiences late spring and summer GEM concentrations that are significantly higher than the hemispheric background (Steffen et al., 2005). These high values can be analogously defined as atmospheric mercury emission events (AMEEs), however, the mechanism for AMEEs is not well understood. They do tend to coincide with melt conditions (Dommergue et al., 2003), so there is certainly potential for their occurrence to be affected by climate change and therefore influence the future Arctic mercury budget.

Measurements at Alert, Canada, comprise the longest continuous data set on Arctic atmospheric mercury at 14 yr. Although it is generally accepted that climate-driven trends require at least 30 yr of data coverage to be distinguishable from interannual variability, it is likely that areas which experience more rapid change – such as the Arctic – will also see the trend emerge from the noise on shorter timescales. Therefore, an analysis of atmospheric mercury was undertaken in order to determine if there was a statistical change in concentrations from 1995 to 2007. A previous analysis up to 2005 showed no significant long term trend in the annual GEM concentration at Alert (Temme et al., 2007), but in this paper we extend the analysis in time, use an alternative statistical method, and look at seasonal behaviour in order to isolate the springtime AMDE chemistry. In addition, we examine the relationship between AMDEs and meteorological and climate parameters in this extensive data set and a shorter one from Amderma, Russia, in order to assess whether climate change may be expected to influence future springtime mercury deposition to the Arctic ecosystem.

2   Methods

Measurements of atmospheric gaseous mercury have been obtained using a commercial Tekran 2537A instrument at Alert, Canada (82.50° N, 62.33° W) since 1995 and at Amderma, Russia (69.72° N, 61.62° E) since 2001. The instruments are set up with a 0.2 μm Teflon filter at the outside inlet (47 mm diameter) followed by an approximately 30-foot sample line heated to 50°C to the back of the instrument, which houses an additional identical Teflon filter. Due to the presence of the two filters, the measured concentrations are assumed to represent gaseous elemental mercury based on results from a previous measurement campaign (Steffen et al., 2002). Two gold collectors are used, alternating between collection and analysis cycles every five or 30 min for continuous monitoring. Hourly averages of these data were calculated for this analysis, requiring 25% completeness. The quality control process used for these data sets was the Environment Canada-developed Research Data Management and Quality Assurance System (RDMQ) and follows the protocol for the Canadian Atmospheric Mercury Measurements Network (CAMNet) (Steffen and Schroeder, 1999). GEM measurements at Alert were only valid for the first half of 2008, therefore this analysis was limited to 1995–2007.

Meteorological data from the Global Atmospheric Watch station at Alert – such as temperature, wind speed, and wind direction – were reported as five-minute means which were then averaged to hourly means, using vector averaging in the case of the wind speed and direction. Hourly relative humidity (up to 2006) and global solar radiation (up to 2003) were obtained by request from Environment Canada's Climate Services Branch (Environment Canada). Temperature, wind speed, wind direction, and relative humidity were reported at Amderma approximately every three hours.

Monthly sea ice area index for the Northern Hemisphere was obtained from the National Snow and Ice Data Center records (Fetterer et al., 2002, updated 2009). To approximate the area of seasonal (first-year) sea ice in the spring months, the sea ice area for the previous September was subtracted from the total sea ice area for the

month.

Temporal trends in GEM concentrations by month were calculated using the seasonal Kendall test and seasonal Kendall slope estimator (Gilbert, 1987). This method is an extension of the non-parametric Mann-Kendall test for trend, which is a recommended trend test when there are missing values and where the data are not normally distributed – both of which apply to the Alert data set. In the seasonal method, data from each month are treated separately and a slope is estimated for each month using Sen's nonparametric estimator of slope. For the purposes of these calculations, each hourly data point in the month is treated as a replicate measurement. An overall annual trend can be estimated from the monthly trend statistics; however, this estimate is less reliable if the monthly trends are not sufficiently homogeneous. A test for seasonal homogeneity was therefore performed as well (van Belle and Hughes, 1984).

In the past, depletion events were defined by the ambient GEM concentration dipping below $1.0\,\mathrm{ng\,m^{-3}}$ (Steffen et al., 2002). For the purposes of this analysis, the mean background GEM concentration at Alert, as well as its standard deviation, was calculated from all the September–December hourly averages from all years. This time period was chosen to best represent background mercury concentrations that are minimally affected by spring AMDEs, summer AMEEs, or late winter Arctic Haze buildup, as shown by the relatively low variability in measured GEM. An atmospheric mercury depletion event (AMDE) was then defined as a GEM concentration more than 3.9 standard deviations below this mean, corresponding to the 99.99% confidence limit and thereby minimizing the number of false positives in the classification of a measurement as a depletion event. Similarly, mercury emission events (AMEEs) were defined as measurements more than 3.9 standard deviations above the September–December mean. This calculation resulted in standard cutoff values of $<1.063\,\mathrm{ng\,m^{-3}}$ for AMDEs and $>1.970\,\mathrm{ng\,m^{-3}}$ for AMEEs. These cutoffs implicitly assume a constant September–December GEM concentration, which was acceptable when looking at AMDEs or AMEEs as a function of variables such as temperature, etc. However, when assessing the presence or absence of trends in AMDEs and AMEEs the cut-

offs were adjusted for each year by the calculated trend in the September–December means to give values of, respectively, $1.116\,\text{ng m}^{-3} - (0.0088\,\text{ng m}^{-3}\,\text{yr}^{-1})\cdot(N_{1995})$ and $2.022\,\text{ng m}^{-3} - (0.0088\,\text{ng m}^{-3}\,\text{yr}^{-1})\cdot(N_{1995})$, where N_{1995} is the number of years since 1995.

In order to quantify the combined frequency and strength of depletion (or emission) events, an integrated AMDE quantity was calculated by summing the magnitude of each hourly measurement classified as an AMDE – that is, the difference between the measured value and the cutoff value calculated as described above – and dividing by the total number of hourly measurements, N:

$$\frac{\sum_{i=1}^{N}|C_{\text{AMDEcutoff}} - C_i|}{N}, \text{ where } C_i < C_{\text{AMDEcutoff}} \tag{1}$$

This integrated AMDE frequency thus provides a measure of both the frequency and intensity of depletion events. The analogous calculation for integrated AMEE frequency was also done, using the data points where $C_i > C_{\text{AMEEcutoff}}$. These calculations were performed for measurements grouped by time period (e.g. by month or season), requiring 70% data coverage within the time period, and by meteorological parameters such as a temperature or wind speed range, requiring a minimum of twenty valid hourly measurements. When calculating total springtime integrated AMDEs or AMEEs at Alert, each month was required to have 70% completeness.

3   Results and discussion

3.1   Trends in atmospheric Hg^0 at Alert

The mean GEM concentrations of each month, averaged over 1995–2001 and 2002–2007, are shown in the top of Fig. 1 for illustrative purposes. Only months with at least 70% data completeness were included in the mean. In the bottom of Fig. 1 are

A. S. Cole and A. Steffen

the annual concentration changes calculated using the Sen's slope estimate (based on the seasonal Kendall test for trend) for each month and the 95% confidence limits on the slope. Positive slopes represent an overall increasing trend in the concentration of GEM in that particular month over the period 1995–2007, while negative slopes indicate a decreasing trend. Two major changes in the annual GEM concentration profile are clear from this figure: (1) The spring minimum GEM concentration, driven by depletion event chemistry, has shifted from May to April; and (2) there has been a decrease in the background (fall/winter) GEM concentration at Alert. An overall annual trend of $-0.0086\pm0.0014\,\mathrm{ng\,m^{-3}\,yr^{-1}}$ ($-0.56\%\,\mathrm{yr^{-1}}$) was estimated based on monthly trends in daily mean GEM (which were equivalent to the trends using hourly data but have larger confidence bands), since using hourly data to calculate the annual slopes was not feasible due to the number of data points. The statistical test for seasonal heterogeneity, however, indicates that the monthly trends based on daily or hourly mean GEM values are sufficiently different that the estimated trend for the entire year is not reliable. This can be seen in Fig. 1 as the lack of overlap between error bars of different months. However, monthly trends using a single data point for each month (median monthly GEM) were equivalent to those using hourly or daily values (within error bars), but with much larger statistical uncertainties that resulted in a positive test for seasonal homogeneity and an identical annual trend estimate of $-0.0086\,\mathrm{ng\,m^{-3}\,yr^{-1}}$ with a 95% confidence range of ($-0.0134\,\mathrm{ng\,m^{-3}\,yr^{-1}}$, $-0.0021\,\mathrm{ng\,m^{-3}\,yr^{-1}}$). Therefore, we conclude that despite increasing GEM concentrations in May, the overall GEM concentration at Alert is significantly decreasing by approximately 0.6% yr^{-1}. In addition to changes in the frequency and intensity of depletion events by month, resulting in the observed monthly GEM trends, there was a significant decrease in the total springtime (March–June) integrated AMDEs at Alert. However, there was no significant change in integrated AMEEs during the late spring and summer period (May–August).

The decrease in background GEM over this period represents a change in the balance between sources and sinks of atmospheric mercury in the Arctic. One change could be a decrease in global mercury emissions, since emissions were estimated

A. S. Cole and A. Steffen

to have changed from 1995 to 2000 by −2%, or −0.4% yr^{-1} (Pacyna et al., 2006), comparable to the trend in ambient GEM concentration at Alert. The trend at Alert is also comparable to the decreasing trend of −0.015±0.003 ng m^{-3} yr^{-1} estimated for the period 1996–2004 at Cape Point, South Africa (Slemr et al., 2008). If decreasing
5 emissions are the cause of decreasing GEM concentrations at Alert, this trend may reverse as predicted emissions increases from Asia offset decreases from other regions. Alternately, an overall decrease in air concentrations could also be due to an increase in the total deposition of mercury out of the air. While springtime depletion events do not appear to have increased at Alert, AMDE deposition in other regions of
10 the Arctic or ongoing deposition in other seasons may be increasing, possibly influenced by decreasing ice cover or changes in the oxidative capacity of the Arctic atmosphere. If this increased deposition is occurring, atmospheric concentrations could continue to decrease while input of inorganic mercury to the ecosystem could increase. While a long-term record of total filterable mercury in one Arctic location – at Resolute,
15 Canada – reports a decrease from 1974 to 2000 of approximately 3% yr^{-1} in the summer and fall, which suggests a decrease in mercury deposition over that period in those seasons (Li et al., 2009), this trend is likely dominated by decreases in the late 1970s and 1980s. More recent and widespread data on Arctic mercury deposition trends is needed to determine if this trend is ongoing and regional.
20 The springtime minimum in GEM concentration is due to the atmospheric chemistry of AMDEs (Steffen et al., 2008), thus the observed change in the timing of this minimum could be caused by a number of factors that might affect this chemistry. It is thought that meteorology and climate affect the frequency and length of AMDEs, both directly and through the existence of sea ice (Dastoor et al., 2008; Steffen et al., 2002). For
25 example, these events occur primarily at high latitudes where cold temperatures prevail and are likely sustained by stable inversion layers that prevent mixing with low-halogen, higher-mercury air from aloft, as is predicted for ozone depletion events (Lehrer et al., 2004). Therefore, an examination of the relationships between AMDEs and a number of meteorological and climate parameters was performed to determine if any of these

parameters could explain the observed monthly trends in GEM.

3.2 Correlations of depletion and emission events with meteorological and climate parameters

The frequency and intensity of AMDEs was compared with local temperature, wind speed, and wind direction as well as with sea ice area and climate indices. In the case of high frequency measurements such as the local meteorological conditions, data from all years was binned with respect to the meteorological parameter (temperature, wind speed, or wind direction) and the integrated frequency of depletion events was calculated within each bin as described previously. The results are shown for Alert in Fig. 2 and for Amderma in Fig. 3. Also shown are the mean GEM concentrations for each bin, which incorporate both AMDEs and AMEEs.

In both locations, depletion events were less frequent and/or intense at higher temperatures within each month. In addition, at a given temperature, depletion events increased from earlier to later in the spring, at least until AMDEs began to taper off in June. The AMDEs at both locations disappear once the local temperature is above freezing, consistent with what has been previously observed (Lindberg et al., 2002; Steffen et al., 2005). As can also be seen in Figs. 2 and 3, there were fewer AMDEs at Amderma than at Alert, and they began and ended earlier in the spring, consistent with the lower latitude and warmer temperatures there. However, the trend of decreasing AMDEs and increasing GEM concentrations with warmer temperature is the same at both locations. This trend is consistent with what was expected from experimental and modelling results (Adams et al., 2002; Goodsite et al., 2004; Sander et al., 2006), and suggests that increasing temperatures across the Arctic in the future may decrease the frequency or severity of depletion events, at least in the short term. Previous analysis of ozone depletion events (Tarasick and Bottenheim, 2002) suggested a "threshold" surface temperature for severe depletions around −20°C, below which the generation of bromine radicals – which lead to both ozone and mercury depletion events – is very efficient. The temperature dependence seen here does not exhibit this

Title Page

Abstract | Introduction

Conclusions | References

Tables | Figures

◄ | ►

◄ | ►

Back | Close

Full Screen / Esc

Printer-friendly Version

Interactive Discussion

behaviour, however, the actual temperatures recorded at Alert and Amderma are likely indicative of, but not equal to, the temperatures of the air masses in previous days when the depletion chemistry was likely occurring. As would be expected from the tight correlation between springtime ozone and GEM concentrations, ozone depletion events exhibit similar temperature dependence (not shown), suggesting a common underlying cause – whether halogen radical generation or meteorology. There could also be direct temperature effects in the reactions that oxidize GEM to reactive gas phase mercury (RGM). While experiments in the temperature range 393–448 K showed no temperature dependence of the oxidation of GEM by Br radicals (Grieg et al., 1970), similar studies at the low temperatures seen in the Arctic springtime (e.g. 230–273 K) are lacking, and theoretical calculations of the reaction rate predict an inverse temperature dependence (Goodsite et al., 2004). A detailed comparison of ozone and mercury may lead to a better understanding of the mechanism for the temperature dependence but is complicated by the very different properties of these two species and is, therefore, left for further investigation.

The correlation of AMDEs with wind speed was much weaker than that with temperature, as shown in the middle of Figs. 2 and 3. In general, the integrated AMDE frequency in each wind speed bin was not nearly as variable as the AMDE frequency binned by temperature, and a slight peak at around $5\,\mathrm{m\,s^{-1}}$ for all months at Alert was not echoed at Amderma, where the highest values were observed at the lowest wind speeds for April and May. The relationship with wind speed for April and May at Amderma is consistent with depletion events being sustained by more stable (low wind speed), stratified air masses due to strong temperature inversions (Lehrer et al., 2004), but similar behaviour is not seen at Alert. While temperature inversions might be expected to be more prevalent at colder surface temperatures, the fact that the dependence of GEM concentrations on wind speed is much weaker than the dependence on temperature at both locations suggests that the correlation between temperature and depletion events is not primarily due to stable meteorological conditions sustaining mercury-depleted air masses over the measurement site, but is more likely due to

temperature-dependent chemistry local to or upwind of the sites. This conclusion is supported by the poor correlation between temperature and local wind speed in these data sets. While previous short-term observations in the Antarctic showed a correlation between local temperature and wind speed during an AMDE period (Brooks et al., 2008), hourly (or three-hourly at Amderma) temperature and wind speed at our sampling sites were weakly correlated in March (R^2=0.15 at Amderma, R^2=0.22 at Alert) and showed no correlation during April and May at either site (R^2<0.1).

The relationship between AMDEs and local wind direction was very different between the two sites. At Alert, the integrated AMDE frequency was significantly higher when the wind was approaching from a northerly or northeasterly direction in March, April, and May. This direction corresponds to air masses arriving from the Arctic Ocean and is consistent with previous trajectory studies which found that ozone-depleted air masses (which correlate very well with GEM-depleted air) arriving at Alert in April were most likely to have traversed the Arctic Ocean north of Siberia (Bottenheim and Chan, 2006). Winds from the southwest predominate in the spring due to the "funnelling" of air masses by the topography of Ellesmere Island and therefore represent air that has most recently traversed land and in many cases is descending from the free troposphere. These air masses were not as likely to be depleted in mercury. Although local wind direction is not necessarily a robust representation of the back trajectory of air arriving at Alert, a subset of spring days were chosen to perform 3–10 day back trajectories using the NOAA HYSPLIT model (Draxler and Rolph, 2003) and did show that air masses originating over the Arctic Ocean were generally associated with local winds from the north. Hourly wind direction data, therefore, provided a way to confirm using a large data set (>30 000 points) what was already believed from a more intense trajectory analysis (Bottenheim and Chan, 2006), and extend the comparison to other spring months. In contrast to Alert, AMDEs at Amderma did not exhibit any dependence on local wind direction, suggesting that either they do not consistently originate in one particular region or that the longer-term back trajectories of air arriving at Amderma is not well represented by local wind direction. Therefore, a trajectory-based analysis

may be needed in order to identify the source(s) of AMDEs observed at Amderma.

The relationship between AMEEs at Alert and temperature, wind speed and direction, and month is illustrated in Fig. 4. The integrated AMEE frequency peaked around 0°C in all months, was highest in June and July, and was overall much smaller than the integrated AMDE frequencies for the year. The same temperature dependence was observed at Amderma (not shown), and shows that high GEM concentrations were most common during melt periods, whether due to emissions from snowmelt or due to a pulse of oceanic emissions during the breakup of sea ice. AMEEs also appeared to depend on wind speed and direction, at least in June–August. A peak in AMEEs at the lowest wind speeds suggests that the surface is a source of GEM during these months, such that low mixing conditions tend to maintain high GEM concentrations. The correlation of summer AMEE frequency with wind direction is similar to what is seen with spring AMDEs, that is, higher values when the wind is from the north or northeast. This suggests that during melt conditions the ocean and/or its snow and ice cover are a source of GEM. This idea is supported by Andersson et al. (2008), who observed from the Arctic Ocean that the sea ice can act as a barrier to GEM evasion and that increased GEM concentrations were observed when the sea ice was broken by the research ship (Andersson et al., 2008).

In contrast to temperature, which is reasonably conserved in a transported air mass, other climate-related parameters that are not represented by local data may affect the number of AMDEs observed at a site – for instance, the quantity and type of sea ice encountered by the air mass, or large-scale mixing patterns that influence the source region of air arriving at the site. While these parameters may influence the origin and transport of Hg-poor air masses, it is difficult to compare them with atmospheric mercury concentrations at Alert at high time resolution without knowing the air mass origin and transit time in addition to high-resolution sea ice characteristics. Therefore, in order to address the more general question of whether the interannual variability in AMDEs is related to variability in seasonal or total sea ice, or to large-scale climate patterns that influence transport, monthly averages of sea ice area and climate indices

Full Screen / Esc

Printer-friendly Version

Interactive Discussion

were compared with monthly integrated AMDE frequencies at Alert for each month in which sufficient data were available. The entire period 1995–2007 was used for this comparison. There were not enough months with the required data completeness at Amderma to perform a similar comparison, therefore this analysis is limited to Alert. The results of these comparisons are shown in Table 1. The somewhat significant correlations in March between AMDEs at Alert and both the North Atlantic Oscillation (NAO) Index ($p<0.1$) and the Polar/Eurasia Teleconnection Pattern ($p<0.01$) suggest that there is some influence of circulation patterns on depletion events seen at Alert in early spring, either direct or indirect. These two indices are not independent, and suggest that March AMDEs are more frequent and/or intense in years when the circumpolar vortex is strong (shown by a positive PET). It has previously been found that black carbon levels at Alert in winter (December–March) tend to be higher during the positive phase of the NAO (Sharma et al., 2006) due to increased mixing with mid-latitude source regions. This increased mixing would lead to higher inputs of mercury as well, possibly resulting in shorter or less intense depletion events. The correlation does not extend into other spring months, perhaps because of the breakup of the polar vortex, however since most of the springtime depletion events occur in April and May we must be very cautious in interpreting the relationship as scientifically meaningful. Part of the difficulty of this analysis is the relatively small data set (13 yr), which is further reduced by months in which there were insufficient GEM data to only 9 or 10 data points. Additional years of monitoring would allow for a more robust comparison.

Also shown in Table 1 are the correlations between the mean monthly temperatures at Alert and the integrated AMDE frequency. These correlations are not significant ($p>0.2$), despite the significant correlations that do exist when looking at hourly measurements (e.g., top of Fig. 2). This suggests that AMDEs in a given month are related to the distribution of temperatures more than the monthly mean temperature. As a result, it would be difficult to predict the effect of future temperature increases on AMDEs, since an increase in the mean monthly temperature could also feasibly be accompanied by a wider distribution of temperatures, and therefore an increase in extremely

Temperature effects on Arctic gaseous mercury

A. S. Cole and A. Steffen

cold days that are associated with increased AMDE activity. This is discussed further in Sect. 3.3. It is also likely that additional parameters that are not addressed by this analysis are also important drivers of AMDE frequency. For example, while radiative flux is somewhat represented by the julian day (or month, broadly), interannual variability in cloudiness may influence the photochemical generation of halogen radicals. However, this effect would be most important in the region where generation of these radicals take place and would not necessarily relate to radiation levels at Alert. Finally, as previously discussed, it may be that total Northern Hemisphere seasonal sea ice (or Arctic Ocean sea ice, which also showed no relationship to AMDEs) is not a good representation of seasonal ice in the region(s) where AMDEs at Alert originate. Future detailed analysis of higher-resolution sea ice conditions, particularly now that seasonal sea ice area can be more accurately estimated from satellite scatterometer data (Nghiem et al., 2006), may reveal a clearer relationship with AMDEs at Alert once a longer data set is collected.

Finally, to assess the robustness of the relationship between hourly springtime GEM concentration and various parameters, a multiple linear regression was performed and used to predict GEM concentrations for March–June 2008. Temperature alone was able to explain only 16% of the variance in the 1995–2007 data (R^2=0.16), while using both temperature and Julian day (which incorporates the observed dependence on month and serves as a proxy for radiation levels) explained 22% of the variance. Adding wind speed and the cosine of the wind direction (representing the northerly component) as independent variables improved the fit slightly, with this four-parameter model explaining 26% of the variance, but adding solar radiation, sea ice area, and daily NAO index as additional parameters did not improve the fit any further. Therefore, a two-parameter fit using temperature and Julian day was chosen to predict 2008 springtime GEM values. The results of this prediction are compared with measured values in Fig. 5. As would be expected based on the total R^2 of the regression (0.22), much of the variance in the measured concentration is lost in the model. However, this simple two-parameter linear fit does exhibit an ability to predict the timing – though not

Temperature effects on Arctic gaseous mercury

A. S. Cole and A. Steffen

the magnitude – of some of the observed fluctuations in the GEM concentration. This provides an indication that the relationship between temperature, month, and depletion events derived from 1995–2007 data is robust for 2008 as well, though clearly, other parameters that are not accounted for in our analysis account for a large part of the total variance. More sophisticated models of mercury chemistry in the Arctic may possibly be improved, then, by parametrizing the temperature dependence found in this analysis.

3.3 Qualitative comparison of trends

Although local temperature has a significant relationship with depletion events, the overall springtime trends in temperature, as shown in Fig. 6, are not completely consistent with springtime GEM trends (Fig. 1). Decreased GEM concentrations in February, March, and April are consistent with decreased temperatures in those months, but the temperature in May has also decreased slightly from 1995 to 2007 while GEM has increased. It is possible that the inconsistency in the May temperature and GEM trends, as well as the lack of correlation in monthly means discussed in Sect. 3.2, is due to the influence of other factors. For example, changes in incoming radiation or winds arriving from the north could be enough to overwhelm the relatively small change in temperature. However, further analysis reveals that despite the overall decreasing trend in May temperature, the percentage of hourly measurements below $-15\degree C$ – i.e. at temperatures that exhibit strong and frequent AMDEs – was 28% for 1995–2001 and only 21% for 2002–2007. In this case, although the mean temperature decreased, the distribution of temperatures was narrower, resulting in fewer low temperature extremes and fewer (or less intense) AMDEs. The same was not true of the temperature distributions in March and April, which were uniformly shifted to lower temperatures during the period, consistent with increased AMDE frequency. Therefore, the shift in the annual GEM minimum shown in Fig. 1 is consistent with changes in air temperature over the period 1995–2007, though contributions from other factors are also likely.

4 Conclusions

Atmospheric elemental mercury measurements at Alert, Canada, show a significant decrease in local GEM concentration over the period 1995–2007 in every month except May, resulting in an annual trend of $-0.0086\pm0.0014\,\mathrm{ng\,m^{-3}\,yr^{-1}}$. This is the first time that a significant trend has been reported at this long-term monitoring site. It is also shown that mercury depletion events have shifted to earlier in the spring during the last thirteen years.

The results presented here provide additional information about the conditions for both low and high concentrations of atmospheric mercury based on multi-year high-resolution observations. A month-by-month analysis revealed a robust correlation between local temperature and depletion events at both Alert and Amderma, Russia. While this correlation could indicate a potential decrease in AMDEs with increasing temperatures in the future, until the mechanism for the temperature effect is known this correlation is primarily useful as a guide to refining the parametrization of AMDEs in models. We must be very cautious in extending that relationship into future Arctic conditions that deviate significantly from what has been experienced in recent history.

Other parameters, such as local wind speed, total sea ice area, and climate indices, did not correlate with AMDEs at either location, with the exception of a correlation between the March Polar/Eurasian Teleconnection Pattern and AMDEs at Alert that may be due to higher inputs of atmospheric mercury from midlatitudes during years with a weak polar vortex. Wind direction was an important factor in both depletion and emission events observed at Alert but not at Amderma.

Further research into the mechanism of the temperature effect in AMDEs and AMEEs would be valuable for providing models with the tools to predict the effect of climate change on Arctic mercury. For example, while the good correlation between AMDEs and ozone depletion events suggests that the temperature dependence seen in AMDEs is due to a common factor, such as higher levels of halogen radicals at lower temperatures, temperature-dependent laboratory studies of mercury oxidation reac-

tions would quantify (or rule out) any effect of temperature on mercury concentrations separate from those of ozone. Differences in the temperature of maximum integrated AMDE frequency at Alert and Amderma, as well as the relationship between AMDEs at measurement sites and differences in regional ice conditions, could be investigated using a trajectory study similar to what has been done for ozone (Bottenheim and Chan, 2006) that incorporates the past temperature history of air parcels. Finally, the origin of AMEEs is a current knowledge gap, and it is hoped that the dependence on meteorological conditions reported here may motivate further research into their source and mechanism.

References

Adams, J. W., Holmes, N. S., and Crowley, J. N.: Uptake and reaction of HOBr on frozen and dry NaCl/NaBr surfaces between 253 and 233 K, Atmos. Chem. Phys., 2, 79–91, 2002, http://www.atmos-chem-phys.net/2/79/2002/.

Andersson, M. E., Sommar, J., Gardfeldt, K., and Lindqvist, O.: Enhanced concentrations of dissolved gaseous mercury in the surface waters of the Arctic Ocean, Mar. Chem., 110, 190–194, 2008.

Ariya, P., Dastoor, A., Amyot, M., Schroeder, W., Barrie, L., Anlauf, K., Raofie, F., Ryzhkov, A., Davignon, D., Lalonde, J., and Steffen, A.: The Arctic: A sink for mercury, Tellus B, 56, 397–403, 2004.

Bottenheim, J. and Chan, E.: A trajectory study into the origin of spring time Arctic boundary layer ozone depletion, J. Geophys. Res.-Atmos, 111, D19301, doi:10.1029/2006JD007055, 2006.

Full Screen / Esc

Printer-friendly Version

Interactive Discussion

Brooks, S., Lindberg, S., Southworth, G., and Arimoto, R.: Springtime atmospheric mercury speciation in the McMurdo, Antarctica coastal region, Atmos. Environ., 42, 2885–2893, 2008.

Christensen, J. H., Brandt, J., Frohn, L. M., and Skov, H.: Modelling of mercury in the Arctic with the Danish Eulerian Hemispheric Model, Atmos. Chem. Phys., 4, 2251–2257, 2004, http://www.atmos-chem-phys.net/4/2251/2004/.

Cosimo, J. C.: Arctic warming signals from satellite observations, Weather, 61, 70–76, 2006.

Dastoor, A. P., Davignon, D., Theys, N., van Roozendael, M., Steffen, A., and Ariya, P. A.: Modeling dynamic exchange of gaseous elemental mercury at polar sunrise, Environ. Sci. Technol., 42, 5183–5188, 2008.

Dommergue, A., Ferrari, C., Gauchard, P.-A., Boutron, C. F., Poissant, L., Pilote, M., Jitaru, P., and Adams, F. C.: The fate of mercury species in a sub-arctic snowpack during snowmelt, Geophys. Res. Lett., 30, 1621, doi:10.1029/2003GL017308, 2003.

Draxler, R. R. and Rolph, G. D.: HYSPLIT (HYbrid Single-Particle Lagrangian Integrated Trajectory) Model access via NOAA ARL READY Website (http://www.arl.noaa.gov/HYSPLIT.php). Silver Spring, MD, NOAA Air Resources Laboratory, 2003.

Environment Canada. Climate Services: http://www.climate.weatheroffice.ec.gc.ca/, access: July 2008.

Fan, S.-M. and Jacob, D. J.: Surface ozone depletion in Arctic spring sustained by bromine reactions on aerosols, Nature, 359, 522–524, 1992.

Fetterer, F., Knowles, K., Meier, W., and Savoie, M. Sea Ice Index: http://nsidc.org/data/g02135.html, access: 2009 Boulder, CO, National Snow and Ice Data Center, 2002, updated 2009.

Gilbert, R. O.: Statistical Methods for Environmental Pollution Monitoring, Van Nostrand Reinhold Company, New York, 204–240 pp., 1987.

Goodsite, M. E., Plane, J. M. C., and Skov, H.: A theoretical study of the oxidation of Hg^0 to $HgBr_2$ in the troposphere, Environ. Sci. Technol., 38, 1772–1776, 2004.

Grieg, G., Gunning, H. E., and Strausz, O. P.: Reactions of metal atoms. II. The combination of mercury and bromine atoms and the dimerization of HgBr, J. Chem. Phys., 52, 3684–3690, 10.1063/1.1673544, 1970.

Kaleschke, L., Richter, A., Burrows, J. P., Afe, O., Heygster, G., Notholt, J., Rankin, A. M., Roscoe, H. K., Hollwedel, J., Wagner, T., and Jacobi, H.-W.: Frost flowers on sea ice as a source of sea salt and their influence on tropospheric halogen chemistry, Geophys. Res. Lett., 31, L16114, doi:16110.11029/12004GL020655., 2004.

Temperature effects on Arctic gaseous mercury

A. S. Cole and A. Steffen

Title Page

Abstract | Introduction

Conclusions | References

Tables | Figures

◄ | ►

◄ | ►

Back | Close

Full Screen / Esc

Printer-friendly Version

Interactive Discussion

Lehrer, E., Hönninger, G., and Platt, U.: A one dimensional model study of the mechanism of halogen liberation and vertical transport in the polar troposphere, Atmos. Chem. Phys., 4, 2427–2440, 2004,
http://www.atmos-chem-phys.net/4/2427/2004/.

5 Li, C., Cornett, J., Willie, S., and Lam, J.: Mercury in Arctic air: The long-term trend, Sci. Total Environ., 407, 2756–2759, 2009.

Lindberg, S. E., Brooks, S., Lin, C. J., Scott, K. J., Landis, M. S., Stevens, R. K., Goodsite, M. E., and Richter, A.: Dynamic oxidation of gaseous mercury in the Arctic troposphere at polar sunrise, Environ. Sci. Technol., 36, 1245–1256, 2002.

10 Nghiem, S. V., Chao, Y., Neumann, G., Li, P., Perovich, D. K., Street, T., and Clemente-Colon, P.: Depletion of perennial sea ice in the East Arctic Ocean, Geophys. Res. Lett., 33, L17501, doi:10.1029/2006GL027198, 2006.

Pacyna, E. G., Pacyna, J. M., Steenhuisen, F., and Wilson, S.: Global anthropogenic mercury emission inventory for 2000, Atmos. Environ., 40, 4048–4063, 2006.

15 Piot, M. and von Glasow, R.: The potential importance of frost flowers, recycling on snow, and open leads for ozone depletion events, Atmos. Chem. Phys., 8, 2437–2467, 2008,
http://www.atmos-chem-phys.net/8/2437/2008/.

Sander, R., Burrows, J., and Kaleschke, L.: Carbonate precipitation in brine – a potential trigger for tropospheric ozone depletion events, Atmos. Chem. Phys., 6, 4653–4658, 2006,
20 http://www.atmos-chem-phys.net/6/4653/2006/.

Schroeder, W. H., Anlauf, K. G., Barrie, L. A., Lu, J. Y., Steffen, A., Schneeberger, D. R., and Berg, T.: Arctic springtime depletion of mercury, Nature, 394, 331–332, 1998.

Sharma, S., Andrews, E., Barrie, L. A., Ogren, J. A., and Lavoué, D.: Variations and sources of the equivalent black carbon in the high Arctic revealed by long-term observations at Alert and
25 Barrow: 1989–2003, J. Geophys. Res.-Atmos., 111, D14208, doi:10.1029/2005JD006581, 2006.

Simpson, W. R., Alvarez-Aviles, L., Douglas, T. A., and Sturm, M.: Halogens in the coastal snow pack near Barrow, Alaska: Evidence for active bromine air-snow chemistry during springtime, Geophys. Res. Lett., 32, L04811, doi:10.1029/2004GL021748, 2005.

30 Simpson, W. R., Carlson, D., Hönninger, G., Douglas, T. A., Sturm, M., Perovich, D., and Platt, U.: First-year sea-ice contact predicts bromine monoxide (BrO) levels at Barrow, Alaska better than potential frost flower contact, Atmos. Chem. Phys., 7, 621–627, 2007,
http://www.atmos-chem-phys.net/7/621/2007/.

Temperature effects on Arctic gaseous mercury

A. S. Cole and A. Steffen

Skov, H., Christensen, J. H., Heidam, N. Z., Jensen, B., Wahlin, P., and Geernaert, G.: Fate of elemental mercury in the Arctic during atmospheric depletion episodes and the load of atmospheric mercury to the Arctic, Environ. Sci. Technol., 38, 2373–2382, 2004.

Slemr, F., Brunke, E.-G., Labuschagne, C., and Ebinghaus, R.: Total gaseous mercury concentrations at the Cape Point GAW station and their seasonality, Geophys. Res. Lett., 35, L11807, doi:10.1029/2008GL033741, 2008.

Steffen, A. and Schroeder, W. Standard operating procedures manual for total gaseous mercury measurements: Canadian Atmospheric Mercury Measurements Network (CAMNet), Toronto, Canada, Environment Canada, 1999.

Steffen, A., Schroeder, W., Bottenheim, J., Narayan, J., and Fuentes, J.: Atmospheric mercury concentrations: measurements and profiles near snow and ice surfaces in the Canadian Arctic during Alert 2000, Atmos. Environ., 36, 2653–2661, 2002.

Steffen, A., Schroeder, W., Macdonald, R., Poissant, L., and Konoplev, A.: Mercury in the Arctic atmosphere: An analysis of eight years of measurements of GEM at Alert (Canada) and a comparison with observations at Amderma (Russia) and Kuujjuarapik (Canada), Sci. Total Environ., 342, 185–198, 2005.

Steffen, A., Douglas, T., Amyot, M., Ariya, P., Aspmo, K., Berg, T., Bottenheim, J., Brooks, S., Cobbett, F., Dastoor, A., Dommergue, A., Ebinghaus, R., Ferrari, C., Gardfeldt, K., Goodsite, M. E., Lean, D., Poulain, A. J., Scherz, C., Skov, H., Sommar, J., and Temme, C.: A synthesis of atmospheric mercury depletion event chemistry in the atmosphere and snow, Atmos. Chem. Phys., 8, 1445–1482, 2008, http://www.atmos-chem-phys.net/8/1445/2008/.

Tarasick, D. W. and Bottenheim, J. W.: Surface ozone depletion episodes in the Arctic and Antarctic from historical ozonesonde records, Atmos. Chem. Phys., 2, 197–205, 2002, http://www.atmos-chem-phys.net/2/197/2002/.

van Belle, G. and Hughes, J. P.: Nonparametric tests for trend in water quality, Water Resour. Res., 20, 127–136, 1984.

Vogt, R., Crutzen, P. J., and Sander, R.: A mechanism for halogen release from sea-salt aerosol in the remote marine boundary layer, Nature, 383, 327–330, 1996.

Temperature effects on Arctic gaseous mercury

A. S. Cole and A. Steffen

Title Page

Abstract	Introduction
Conclusions	References
Tables	Figures

|◄ | ►|

◄ | ►

Back | Close

Full Screen / Esc

Printer-friendly Version

Interactive Discussion

Table 1. Pearson's correlation coefficients (R), and statistical significance level (p), expressed as R (p), for monthly integrated AMDEs at Alert with monthly climate-related parameters. The number of months in the period 1995–2007 with sufficient GEM data are reported as N.

	March ($N=9$)	April ($N=9$)	May ($N=9$)	June ($N=10$)
Northern Hemisphere sea ice area	−0.54 (0.14)	−0.27 (0.48)	0.52 (0.15)	0.46 (0.18)
Northern Hemisphere seasonal sea ice area (estimated)	0.14 (0.72)	−0.05 (0.89)	−0.25 (0.52)	0.21 (0.57)
Arctic Oscillation Index	0.44 (0.24)	−0.11 (0.78)	−0.35 (0.36)	0.04 (0.90)
North Atlantic Oscillation Index	−0.61 (0.08)	−0.34 (0.37)	0.50 (0.18)	−0.07 (0.85)
Polar/Eurasia Teleconnection Pattern (PET)	0.84 (0.005)	0.14 (0.37)	−0.45 (0.23)	0.05 (0.90)
Mean monthly temperature	−0.44 (0.24)	−0.02 (0.96)	−0.41 (0.27)	0.43 (0.22)
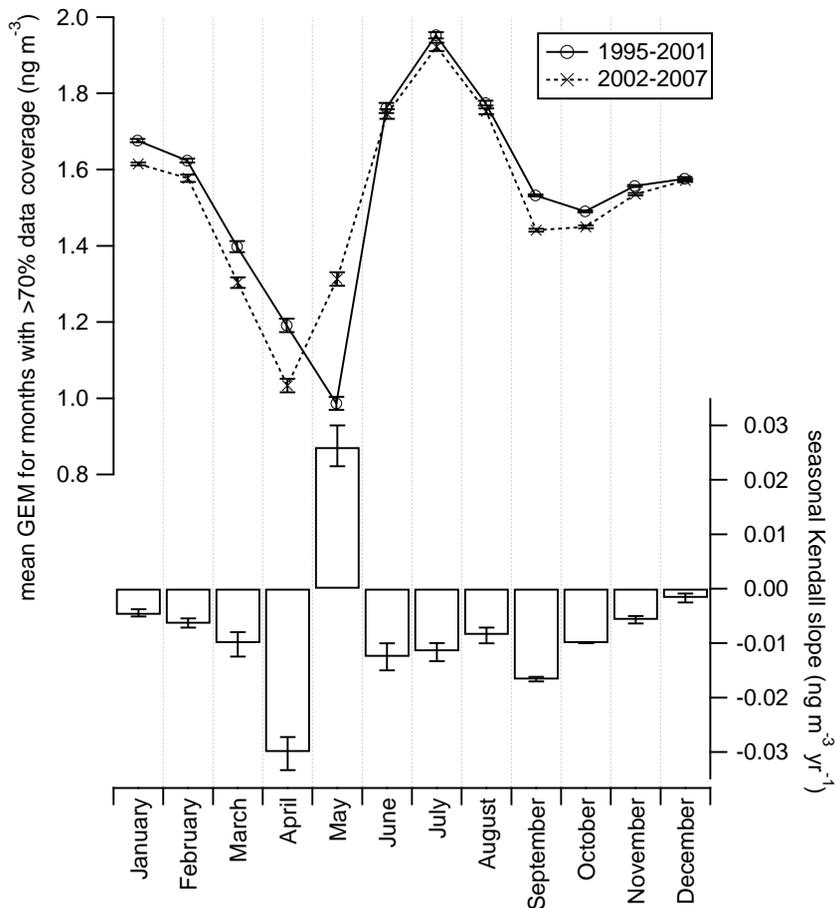
Fig. 1. Seasonal profiles of gaseous elemental mercury concentrations at Alert for 1995–2001 and 2002–2007 (top); change in concentration with time calculated for each month by Sen's estimator of slope (bottom).

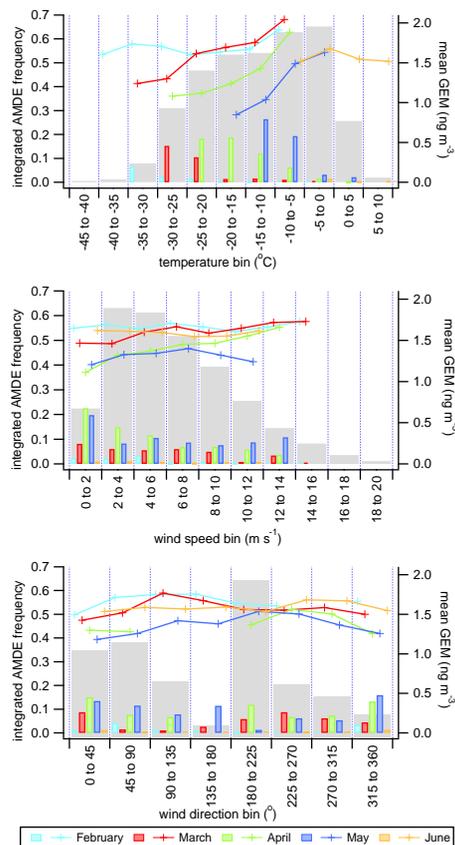**Temperature effects on Arctic gaseous mercury**

A. S. Cole and A. Steffen
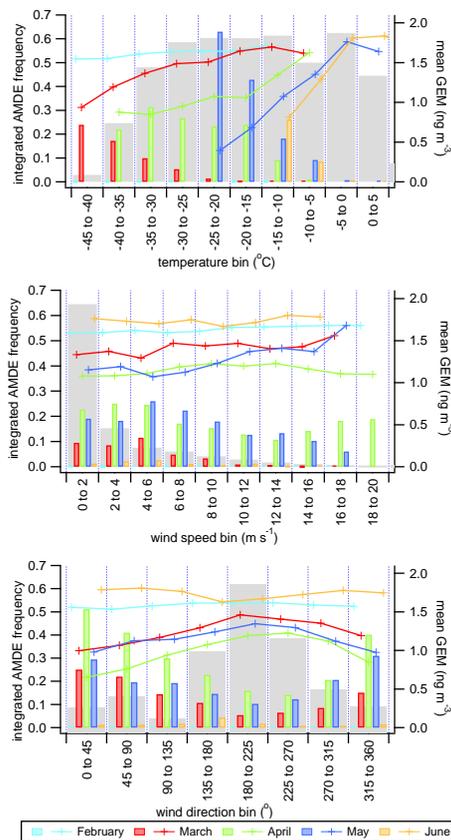
Fig. 2. Integrated AMDE frequency (coloured bars) and mean gaseous elemental mercury (lines), as a function of temperature, wind speed, wind direction and month for Alert data 1995–2007. For reference, springtime frequency histograms of the observed meteorological parameters are included in gray.

Temperature effects on Arctic gaseous mercury

A. S. Cole and A. Steffen

Title Page

Abstract | Introduction

Conclusions | References

Tables | Figures

|◄ | ►|

◄ | ►

Back | Close

Full Screen / Esc

Printer-friendly Version

Interactive Discussion

Fig. 3. Integrated AMDE frequency (coloured bars) and mean gaseous elemental mercury (lines), as a function of temperature, wind speed, wind direction and month for Amderma data 2001–2007. For reference, springtime frequency histograms of the observed meteorological parameters are included in gray.
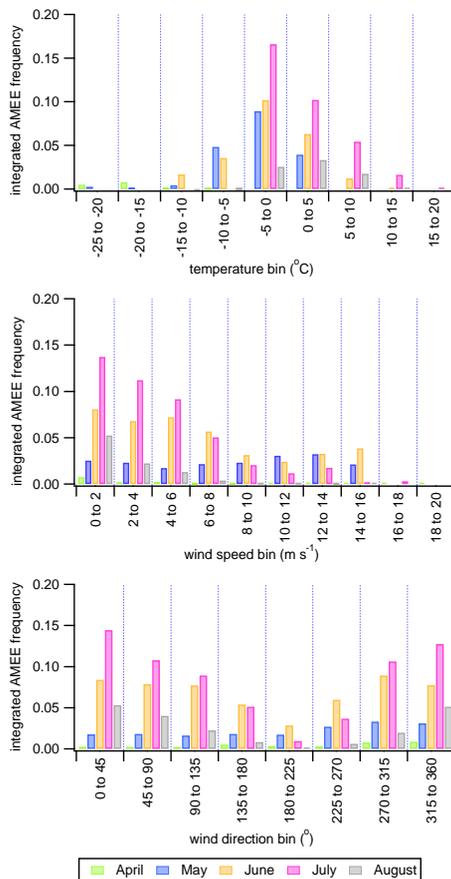
Fig. 4. Integrated AMEE frequency as a function of temperature, wind speed, wind direction and month for Alert data 1995–2007. Note the change in scale from Figs. 2 and 3.
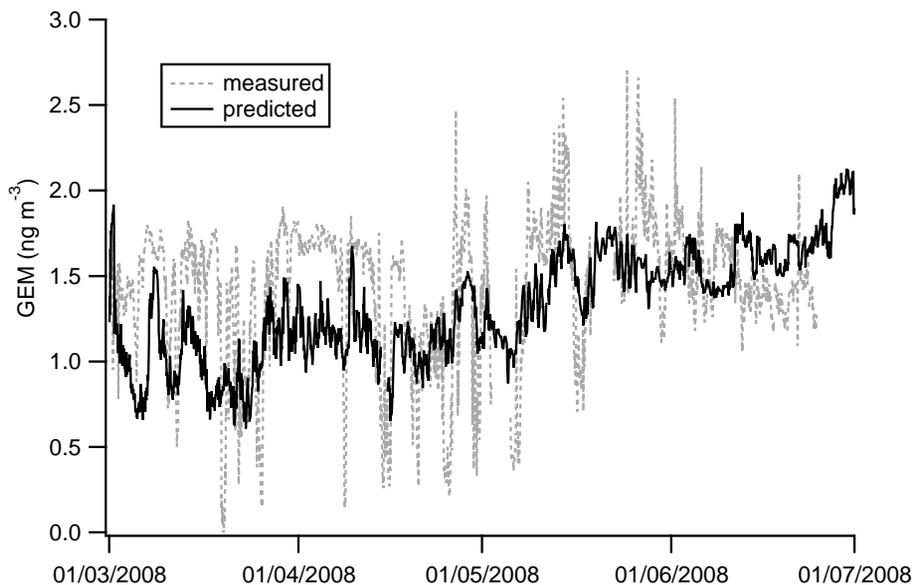
Fig. 5. Comparison of measured hourly GEM concentrations at Alert for March–June 2008 with those predicted based on a multiple linear regression fit of 1995–2007 GEM concentrations to local temperature and Julian day.
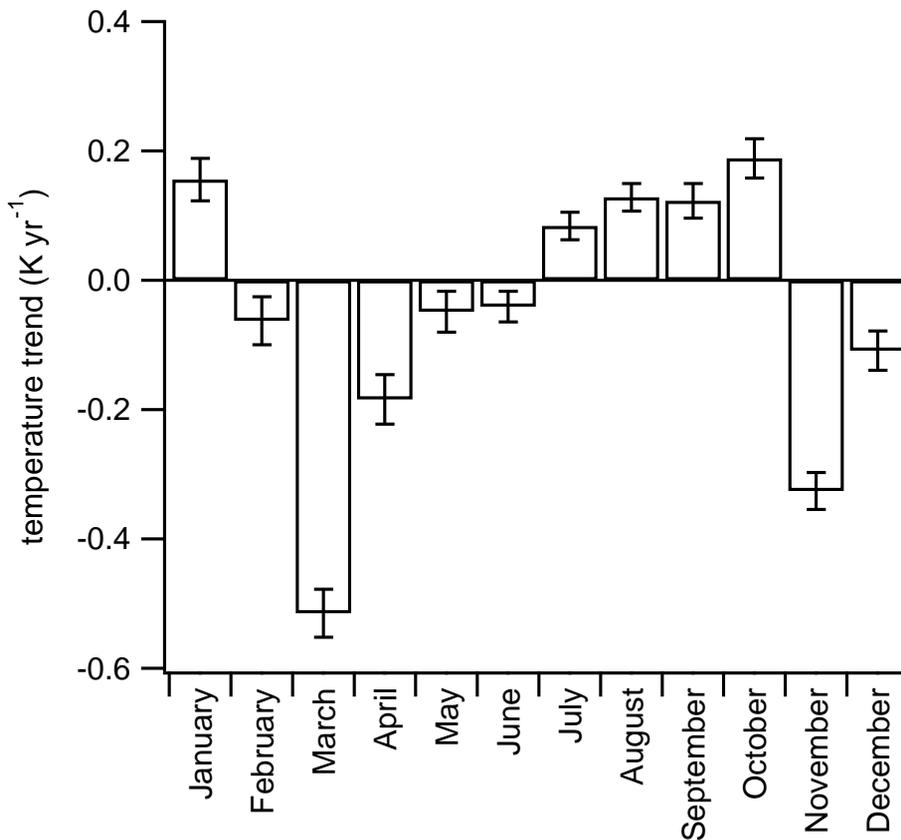
Fig. 6. 1995–2007 trends in local temperature at Alert calculated for each month by Sen's estimator of slope.